

Selective and Reversible Inhibition of Active CO₂ Transport by Hydrogen Sulfide in a Cyanobacterium¹

George S. Espie^{*2}, Anthony G. Miller, and David T. Canvin

Department of Biology, Queen's University, Kingston, Ontario, Canada K7L 3N6

ABSTRACT

The active transport of CO₂ in the cyanobacterium *Synechococcus* UTEX 625 was inhibited by H₂S. Treatment of the cells with up to 150 micromolar H₂S + HS⁻ at pH 8.0 had little effect on Na⁺-dependent HCO₃⁻ transport or photosynthetic O₂ evolution, but CO₂ transport was inhibited by more than 90%. CO₂ transport was restored when H₂S was removed by flushing with N₂. At constant total H₂S + HS⁻ concentrations, inhibition of CO₂ transport increased as the ratio of H₂S to HS⁻ increased, suggesting a direct role for H₂S in the inhibitory process. Hydrogen sulfide does not appear to serve as a substrate for transport. In the presence of H₂S and Na⁺-dependent HCO₃⁻ transport, the extracellular CO₂ concentration rose considerably above its equilibrium level, but was maintained far below its equilibrium level in the absence of H₂S. The inhibition of CO₂ transport, therefore, revealed an on-going leakage from the cells of CO₂ which was derived from the intracellular dehydration of HCO₃⁻ which itself had been recently transported into the cells. Normally, leaked CO₂ is efficiently transported back into the cell by the CO₂ transport system, thus maintaining the extracellular CO₂ concentration near zero. It is suggested that CO₂ transport not only serves as a primary means of inorganic carbon acquisition for photosynthesis but also serves as a means of recovering CO₂ lost from the cell. A schematic model describing the relationship between the CO₂ and HCO₃⁻ transport systems is presented.

Cyanobacteria possess mechanisms for the active transport of CO₂ and HCO₃⁻ that lead to the accumulation of a large intracellular pool of DIC³ (2, 6, 10, 11, 13, 16, 17, 28) which serves as the immediate source of CO₂ for photosynthesis (10, 16). During steady state photosynthesis in *Synechococcus leopoliensis* UTEX 625 both species of DIC are transported simultaneously and continuously in light dependent processes (7). Although cyanobacteria rapidly remove CO₂ from the medium (2, 7, 17, 28), it is HCO₃⁻ transport which provides the bulk of the DIC to the intracellular pool when the extracellular pH is alkaline and the [DIC] low (2, 6, 7, 10, 16). Transport of HCO₃⁻ by air-grown cells of *Synechococcus* (6,

8, 13, 20) and *Anabaena variabilis* (11) requires extracellular Na⁺, with an optimum [Na⁺] of around 25 mM for *Synechococcus* cells at pH 8. The active transport of CO₂ by air-grown cells of *Synechococcus* also requires Na⁺ (8, 14, 17), but the optimum [Na⁺] for this process is around 100 μM. At pH 8, the differential requirement for Na⁺ provides a convenient means to distinguish between the two transport processes.

Analysis of the roles of CO₂ and HCO₃⁻ transport in photosynthesis would be further facilitated by an ability to selectively inhibit CO₂ transport. To this end, several groups have reported that the CA inhibitor EZ inhibits CO₂ transport in *Anabaena variabilis* (1, 28). However, the results of a recent study by Price and Badger (25) using *Synechococcus* PCC 7942 suggests that EZ, at 200 μM, equally inhibits CO₂ and HCO₃⁻ transport.

We have recently found that COS, an isoelectronic structural analog of CO₂, inhibits active CO₂ transport in *Synechococcus* UTEX 625 and that it is also an alternate substrate for the transport system (19). The use of COS, however, is complicated by the fact that it is broken down by CA or by intact cyanobacterial cells to CO₂ and H₂S (19). In this paper we demonstrate that H₂S is also a potent, selective, and reversible inhibitor of active CO₂ transport in the cyanobacterium *Synechococcus* UTEX 625.

MATERIALS AND METHODS

Organisms and Growth

The unicellular cyanobacterium *Synechococcus leopoliensis* UTEX 625 (University of Texas Culture Collection, Austin, TX) was grown with air-bubbling (0.05% v/v CO₂) in unbuffered Allen's medium at 30°C as described previously (6).

Experimental Conditions

Cells were washed three times by centrifugation (1 min at 10,000g, Beckman microfuge B) and resuspended (7–9 μg Chl·mL⁻¹) in 25 mM BTP/HCl buffer of the appropriate pH. The buffer contained about 15 μM DIC and 5 μM Na⁺ as contaminants. Washed cells (6 mL) were subsequently placed in a thermostated (30°C) glass reaction vessel (20 mm diameter) and briefly purged with a stream of N₂ to reduce the [O₂] to less than 75 μM. The chamber was then closed to the atmosphere and the cells were allowed to temperature equilibrate for several minutes in darkness. The reaction vessel contained a port for the inlet capillary of a mass spectrometer and the cell suspension was continuously stirred with a magnetic stirrer during measurements. Light was provided by a

¹ Supported by grants from the National Sciences and Engineering Research Council of Canada (NSERC) to D. T. C. and an NSERC postdoctoral fellowship to G. S. E.

² Present address: Department of Biology, Concordia University, Montreal, Quebec, Canada H3G 1M8.

³ Abbreviations: DIC, dissolved inorganic carbon (CO₂ + HCO₃⁻ + CO₃²⁻); BTP, 1,3-bis (tris [hydroxymethyl] methylamino)-propane; CA, carbonic anhydrase; EZ, ethoxazolamide; F_M, maximum fluorescence yield; F_V, variable fluorescence.

tungsten-halogen projector lamp with $210 \mu\text{E} \cdot \text{m}^{-2} \cdot \text{s}^{-1}$ incident upon the front surface of the reaction vessel. The [Chl] of cell suspensions was determined spectrophotometrically at 665 nm after extraction in methanol (6). The pH of cell suspensions was measured with a Ross combination glass pH electrode connected to an Orion 701 pH meter and did not change by more than 0.03 units during the course of an experiment.

Mass Spectrometry

The concentration of dissolved O_2 , H_2S , $^{12}\text{CO}_2$, or $^{13}\text{CO}_2$ ($m/e = 32, 34, 44$, and 45 , respectively) in cell suspensions was determined with a magnetic sector mass spectrometer (VG Gas Analysis, Middlewich, England; model MM 14-80 SC) equipped with a membrane inlet system (7, 17). The output signal from the mass spectrometer was directed to an external amplification/attenuation and frequency-cutoff unit and subsequently to a Fisher Recordall 5000 strip chart recorder. The response time (63% full response) of the measuring system was about 2 s. The mass spectrometer was calibrated for CO_2 and O_2 as described previously (7, 17). The mass spectrometer was calibrated for H_2S by monitoring the increase in the signal at mass 34 after injection of a known volume of a Na_2S solution into 6 mL of 25 mM BTP/HCl buffer (pH 8.0) contained in the mass spectrometer reaction vessel.

Preparation of Na_2S and CO_2 Stock Solutions

Stock solutions of $\text{Na}_2\text{S} \cdot 9 \text{H}_2\text{O}$ (BDH, Toronto) were prepared fresh daily and stored under N_2 . Large white crystals of this hygroscopic compound were quickly washed with distilled H_2O , blotted dry, weighed, and dissolved in deoxygenated distilled H_2O . Near complete dissociations of Na_2S occurs yielding a basic ($\text{pH} > 9$) solution in which HS^- is the predominant sulfur-containing species (9). The concentration of HS^- was determined spectrophotometrically at 230 nm using a molar absorption coefficient of $7762 \text{ L} \cdot \text{mol}^{-1} \cdot \text{cm}^{-1}$ (9) and was found to be within 5% of the value expected. The reaction $\text{H}_2\text{S} \rightarrow \text{H}^+ + \text{HS}^-$ has a pK_a of 6.91 at 30°C and infinite dilution (21) and this value was used to calculate the concentration of H_2S and HS^- in buffers of varying pH.

Aqueous solutions of CO_2 were prepared by continuously bubbling acidified (2 mM HCl) ice-cold distilled H_2O with 5% v/v CO_2 . The CO_2 concentration was determined by injecting a 10 to 15 μL sample of the solution into the closed mass spectrometer reaction vessel containing 6 mL of BTP/HCl buffer (pH 8.0), and 25 $\mu\text{g} \cdot \text{mL}^{-1}$ CA. Under these conditions, 1.56% of the added CO_2 remained as such with the rest being rapidly converted to HCO_3^- . The increase in the mass 44 signal was compared to that elicited by a known concentration of K_2CO_3 , and the concentration of the $[\text{CO}_2]$ in the stock solution was calculated and found to be between 3.6 and 3.9 mM.

CO_2 Transport

The ability of *Synechococcus* cells to actively transport CO_2 (as distinct from HCO_3^- transport) was determined in three

different ways. One method involved measuring the decrease in $[\text{CO}_2]$ in solution upon illumination of the cells. A second method, which probed the cells' ability to transport CO_2 under steady-state conditions, involved measuring the disappearance of CO_2 from the illuminated suspension following the addition of a 'pulse' of CO_2 to yield an initial concentration of 2 to 4 μM . The final method involved measuring the increase (if any) in $[\text{CO}_2]$ when the cells were provided with a known [DIC] at the compensation point. The latter two procedures were conducted in the absence and presence of HCO_3^- transport which was initiated by the addition at 25 mM NaCl (6, 8, 13, 20).

Fluorimetry

Changes in Chl *a* fluorescence yield, which occurred as a consequence of DIC transport (15, 18) were measured with a pulse modulation fluorometer described in Schreiber *et al.* (26) (PAM-101, H. Walz, D-8521, Effeltrich, F.R.G.). Actinic light to drive DIC transport and photosynthesis was provided at $210 \mu\text{E} \cdot \text{m}^{-2} \cdot \text{s}^{-1}$. Fluorescence yield was monitored with a weak pulse modulated beam (about $1 \mu\text{E} \cdot \text{m}^{-2} \cdot \text{s}^{-1}$ at 100 kHz). Fluorescence yield was monitored at the same time as CO_2 or O_2 fluxes were being measured with the mass spectrometer by placing one end of the fiber optics system of the fluorometer at the surface of the mass spectrometer reaction cuvette. For *Synechococcus*, the maximum yield of Chl *a* fluorescence (F_M) following a saturating light flash was taken as that occurring at the CO_2 compensation point. F_V was determined as in Miller and Calvin (15).

Chemicals

Carbonic anhydrase and BTP were obtained from Sigma Chemical Co. (St. Louis). Analytical grade $\text{Na}_2\text{S} \cdot 9 \text{H}_2\text{O}$ was obtained from BDH (Toronto) and $\text{K}_2^{13}\text{CO}_3$ (99 atom % ^{13}C) was obtained from MSD Isotopes (Montreal). D^{12}C and ^{13}C stocks were made by dissolving the appropriate quantity of $\text{K}_2^{12}\text{CO}_3$ or $\text{K}_2^{13}\text{CO}_3$ in distilled H_2O . These solutions had a pH above 8 and therefore the DIC was largely in the form of HCO_3^- and CO_3^{2-} . The stocks were used both as a source of DIC for transport and photosynthesis and as calibration standards for the mass spectrometer.

RESULTS

When 25 μM DIC was added to cells in the light at the CO_2 compensation point, in the absence of Na_2S , there was a rapid quenching of Chl *a* fluorescence (Fig. 1A). This quenching was mainly due to HCO_3^- transport (15, 18) since under the conditions employed (pH 8, 25 μM DIC, 25 mM NaCl) the contribution from CO_2 uptake would be limited by the rate of HCO_3^- conversion to CO_2 in the medium. In the absence of 25 mM NaCl virtually no change in fluorescence yield was observed (not shown). The uptake of HCO_3^- by the cells was further indicated by the observation that photosynthesis exceeded by 11.7-fold the CO_2 supply rate (Fig. 1C). That CO_2 transport occurred, however, was shown by the fact that following DIC addition the extracellular $[\text{CO}_2]$ remained near zero and below its equilibrium concentration (Fig. 1B). This

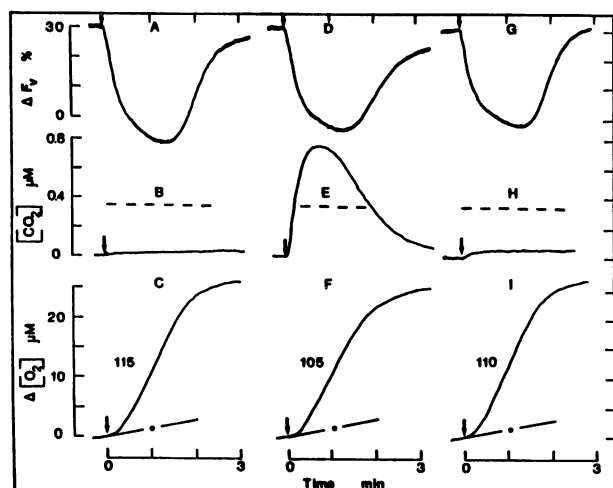


Figure 1. Time dependent changes in Chl *a* fluorescence yield (A, D, G), CO₂ concentration (B, E, H) and photosynthetic O₂ evolution (C, F, I) in the absence (A, B, C) or presence (D, E, F) of 150 μM Na₂S and following the removal of H₂S + HS⁻ from solution by flushing with N₂ (G, H, I). The reaction was started by the addition of 25 μM DIC (↓) to illuminated cells at the compensation point. The dashed lines (---), panels B, E, and H, indicate the CO₂ concentration that would be in equilibrium with 25 μM DIC. The broken lines (— · —), panels C, F, and I, indicate maximum photosynthetic O₂ evolution which could be supported by CO₂ uptake alone. The numbers beside the solid lines (C, F, I) indicate the observed rate of photosynthesis in μmol O₂ · mg⁻¹ Chl · h⁻¹. Changes in fluorescence yield and CO₂ concentration were measured simultaneously. Photosynthetic O₂ evolution (and fluorescence, not shown) was measured in a parallel run with the same cell suspension. Cells (8.0 μg Chl · mL⁻¹) were suspended in 25 mM BTP/HCl buffer (pH 8.0) containing 25 mM NaCl, at 30°C with illumination at 210 μE · m⁻² · s⁻¹.

was true even at the earliest times after DIC addition when substantial HCO₃⁻ remained in the medium (Fig. 1B). The near-zero [CO₂] was also maintained in the face of continuous CO₂ resupply from HCO₃⁻ dehydration, indicating a continuous uptake of CO₂ by the cells (7, 17). This uptake occurred against a considerable concentration gradient for CO₂ (7, 8, 17) indicating that CO₂ was actively transported. The added DIC was ultimately consumed in photosynthesis as indicated by the cessation of O₂ evolution (Fig. 1C) and a return of Chl *a* fluorescence yield to a near-maximum level (Fig. 1A).

When 25 μM DIC was added to cells in the presence of 150 μM Na₂S, the extracellular [CO₂] (Fig. 1E), rather than remaining close to zero (Fig. 1B), rose dramatically to a level considerably in excess of the equilibrium concentration calculated (and measured, not shown) for the DIC initially added. In fact, the extracellular [CO₂] remained above the equilibrium value during much of the experiment, approaching zero only after most of the DIC had been consumed in photosynthesis (Fig. 1F). Although it was evident that the cells' ability to actively transport CO₂ was severely retarded by Na₂S (Fig. 1E), the transport of HCO₃⁻ by the cells, as judged by the yield of Chl *a* fluorescence (Fig. 1D) was only marginally affected. Similarly, photosynthetic O₂ evolution proceeded at 91% of the rate obtained in the absence of Na₂S (Fig. 1, C and F).

As shown by the decline in the mass 34 signal, the H₂S + HS⁻ could be almost completely removed from the cell suspension by purging with N₂ for 1 min. When this was done, the chamber reclosed and 25 μM DIC added, it was again found that extracellular [CO₂] remained near zero, indicating a restoration of CO₂ transport activity (Fig. 1H). Evidently, the inhibition of CO₂ transport was caused by volatile H₂S/HS⁻ and was readily reversible. Fluorescence yield and O₂ evolution following DIC addition was similar to control (Fig. 1, G and I).

An interesting feature of the inhibition of CO₂ transport by Na₂S was that the extracellular [CO₂] rose substantially above the anticipated equilibrium concentration and this obviously requires energy (Figs. 1 and 2). One potential source for metabolic energy input coupled with the intracellular production of CO₂ is the HCO₃⁻ transport system. Air-grown cells of *Synechococcus* require millimolar concentrations of Na⁺ for HCO₃⁻ transport to occur (6, 8, 13, 20). Thus, in the absence of Na⁺ the effect of H₂S/HS⁻ upon the extracellular [CO₂] after DIC addition can be examined without the occurrence of HCO₃⁻ transport. As mentioned previously, the addition of 25 μM DIC to cells in the absence of Na⁺ did not cause significant quenching of Chl *a* fluorescence nor support a substantial rate of O₂ evolution (not shown) and indicated that HCO₃⁻ transport was indeed inhibited. With HCO₃⁻ transport inhibited and the presence of 150 μM H₂S + HS⁻, the addition of 25 μM DIC caused a rise in the extracellular

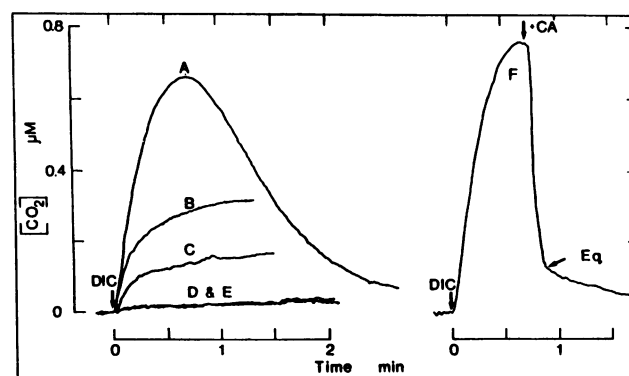


Figure 2. Effect of Na₂S and 25 mM Na⁺ (HCO₃⁻ transport) on the time dependent changes in [CO₂] following the addition of 25 μM DIC (↓) to illuminated suspensions of *Synechococcus* cells at the compensation point. Cells (8.8 μg Chl · mL⁻¹) were suspended in 25 mM BTP/HCl buffer (pH 8.0), in the presence (A, C) or absence (D, E) of 150 μM Na₂S and in the presence (A, D) or absence (C, E) of 25 mM NaCl. Initiation of HCO₃⁻ transport by 25 mM NaCl was confirmed by measurement of Chl *a* fluorescence (not shown). The equilibrium [CO₂] was determined by adding 25 μM DIC to a darkened cell suspension (B, + 25 mM NaCl). To estimate the true extent of the disequilibrium between CO₂ and HCO₃⁻ in cells suspensions containing 150 μM Na₂S and 25 mM NaCl (e.g. curve A), CA (50 μg · mL⁻¹, 125 Wilbur-Anderson units · mL⁻¹) was added at the time (53 s) when the measured [CO₂] was a maximum (curve F). The equilibrium [CO₂] (Eq) was taken as that occurring at the second point of inflection on the curve (F) following CA addition. Since some of the DIC had been consumed in photosynthesis this equilibrium [CO₂] was not expected to correspond to that shown in curve B. The second phase of the decrease in [CO₂] after CA addition was due to photosynthesis.

[CO₂], but to a level which was only about one-half the expected equilibrium [CO₂] (Fig. 2, B and C). In this case, the CO₂ that appeared in the medium probably arose from the extracellular dehydration of HCO₃⁻ and no metabolic energy input was required to yield the measured [CO₂]. The appearance of CO₂ in the medium, however, indicated that CO₂ transport was impaired relative to the control (Fig. 2, D and E) and that Na⁺ *per se* was not required in the inhibition process. In the presence of HCO₃⁻ transport capability (+ 25 mM NaCl) and 150 μM H₂S + HS⁻, the [CO₂] rose substantially above the equilibrium concentration following DIC addition (Fig. 2A). The extent to which the [CO₂] was above the equilibrium concentration (5.8-fold) was established by adding an excess of CA to rapidly equilibrate CO₂ and HCO₃⁻ (Fig. 2F). In other experiments (not shown) K₂¹³CO₃ was added and demonstrated that the added DIC was the source of carbon from which the CO₂ was derived.

The effect of H₂S/HS⁻ on CO₂ transport was further investigated by probing the activity of the transport system with pulses of CO₂ (Fig. 3). The CO₂ provided was initially above the equilibrium value (61.5-fold at pH 8) but the concentration fell rapidly as CO₂ was converted nonenzymatically to HCO₃⁻, in the absence of cells or in darkened cell suspensions (Fig. 3, curve F). Due to the 2 s response time of the mass spectrometer and ongoing CO₂ hydration, a full response to the CO₂ was not observed (Fig. 3, curve F). Thus, no attempt

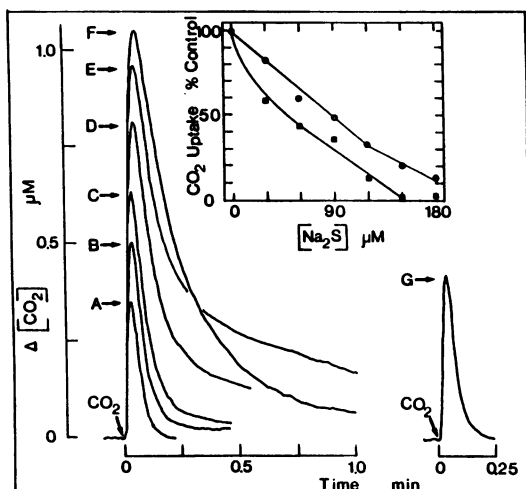


Figure 3. Reversible inhibition of active CO₂ transport. Cells (8.5–9.5 μg Chl·mL⁻¹) suspended in 25 mM BTP/HCl buffer (pH 8) containing 25 mM NaCl were incubated in the light with (A) 0, (B) 30, (C) 60, (D) 90, (E) 180 μM Na₂S. CO₂ transport ability was tested by pulsing the cells with CO₂ contained in a small aliquot of acidified water saturated at 0°C with 5% CO₂ and the changes in [CO₂] in the medium were recorded. The spontaneous decrease in [CO₂], due to conversion to HCO₃⁻, was determined in a darkened cell suspension in the absence of Na₂S (curve F). The accumulated H₂S + HS⁻ (*i.e.* 180 μM) was removed by purging the suspension with N₂ for 2 min and CO₂ transport ability was tested again (curve G). Maximum CO₂ transport the difference in peak height between curve A and F, was set to 100% (Fig. 3, inset). The difference in peak height between experimental curves (+ Na₂S) and the curve obtained in the dark was calculated as percentage of the control level of CO₂ uptake and plotted as function of [Na₂S] (inset). Experiments were conducted either in the presence (●) or absence (■) of 25 mM Na⁺.

was made to calculate rates of CO₂ transport (17). Nevertheless, the method provides an alternate means of assessing CO₂ transport, as distinct from HCO₃⁻ transport, over a range of [CO₂] and is the procedure most directly comparable to ¹⁴CO₂ pulsing techniques used in conjunction with silicone fluid filtering centrifugation (2, 17, 28) and isotopic disequilibrium experiments (6).

The light-dependent transport of CO₂ (Fig. 3, *cf.* curve A to F) was progressively inhibited by increasing concentrations of Na₂S (Fig. 3). The full inhibitory effect of Na₂S was obtained within 15 s of addition (not shown). The inhibition of CO₂ transport was readily reversed following the removal of H₂S + HS⁻ from the cell suspension (Fig. 3, curve G). In six different experiments, 85 to 95% of CO₂ transport activity was recovered after purging the cell suspension with N₂ for 1 to 2 min.

Since CO₂ transport rate cannot be measured with the CO₂ pulsing procedure, uptake of CO₂ was simply estimated as the difference between the peak heights of the treatment and dark control. Maximum uptake of CO₂ occurred in the absence of Na₂S (Fig. 3, curve A) and the difference between the heights of curve A and F was taken as 100%. The effect of [Na₂S] on CO₂ uptake in the presence and absence of 25 mM Na⁺ is shown in the inset of Figure 3. As suggested previously (Fig. 2) CO₂ transport was inhibited by Na₂S both in the presence and absence of 25 mM Na⁺ (HCO₃⁻ transport) (Fig. 3, inset). In fact, Na⁺ appeared to give some protection against Na₂S inhibition of CO₂ transport. This effect of Na⁺ may be related to the enhancement of CO₂ transport which occurs in the presence of micromolar levels of Na⁺ (8, 14, 17). Resolution of this matter, however, must await a more detailed study of the effect of [Na⁺].

Upon illumination, cells capable of efficient CO₂ transport caused the extracellular [CO₂] to drop to almost zero (Fig. 4A). As shown by the addition of CA, however, about 62 μM HCO₃⁻ (in equilibrium with 1 μM CO₂) remained in the medium even though HCO₃⁻ transport was ongoing. In the

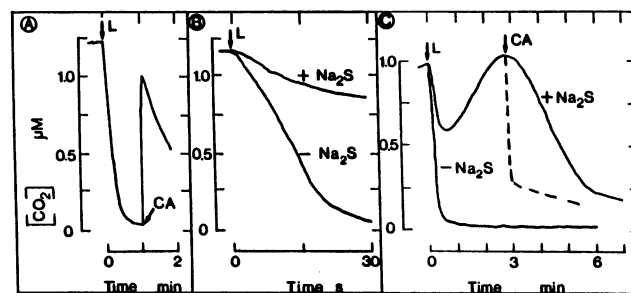


Figure 4. Effect of Na₂S on CO₂ transport initiated by illumination. Cells (8.8 μg Chl·mL⁻¹) were incubated in the dark for several minutes in 25 mM BTP/HCl buffer (pH 8.0) containing 25 mM NaCl, 70 to 100 μM DIC with or without 150 μM Na₂S as indicated. CO₂ transport was initiated by turning on the lights (L). A, Typical time course of CO₂ depletion of the medium by *Synechococcus* following illumination. CA (25 μg·mL⁻¹, 62.5 Wilbur-Anderson units·mL⁻¹) was subsequently added to bring about rapid equilibration between CO₂ and HCO₃⁻. B, Effect of Na₂S on the initial rate of CO₂ depletion following illumination. C, Extended time course of CO₂ depletion of the medium in the presence and absence of Na₂S. In a parallel experiment (---), CA was added (+ Na₂S treatment) at the time when [CO₂] was at a maximum.

presence of Na₂S, the initial uptake of CO₂, upon illumination, was greatly reduced (Fig. 4B). After about 1 min of illumination, an efflux of CO₂ occurred (Fig. 4C) driving the [CO₂] far above its equilibrium value. Eventually the [CO₂] declined to near zero as a consequence of CO₂ fixation supported by Na⁺-dependent HCO₃⁻ transport. The time course of CO₂ uptake and efflux by *Synechococcus* in the presence of Na₂S (Fig. 4C) was very similar to that observed for a marine species of *Synechococcus* in the absence of any added inhibitor (2, 3, 27).

The CO₂ pulsing technique was used to determine whether H₂S or HS⁻ was the species responsible for the inhibition of CO₂ transport. The ratio of H₂S:HS⁻, at constant [Na₂S], was changed by changing the pH of the medium. Figure 5 shows the results of experiments conducted at pH 7 and 8 and at 30 μM Na₂S, along with the appropriate controls. As is evident from the recorder traces, CO₂ transport was inhibited to a much greater extent at pH 7 where 45% of the Na₂S was shown in the form of H₂S. The results of a number of experiments similar to that shown in Figure 5 are summarized in Figure 6. The experiments were conducted over a range of pH from 7.0 to 8.7 ([H₂S]:[HS⁻] = 0.8 to 0.016, respectively) and [Na₂S] from 0 to 200 μM. CO₂ uptake was analyzed as described for Figure 3 and plotted either as a function of [HS⁻] or [H₂S]. When analyzed in this manner the data showed a single inhibition curve for CO₂ uptake with respect to [H₂S] (Fig. 6B), but multiple, pH dependent, curves for [HS⁻]. These data are consistent with H₂S having a central role in the inhibition of active CO₂ transport.

DISCUSSION

Selective Inhibition

Hydrogen sulfide is a potent and reversible inhibitor of active CO₂ transport in the cyanobacterium *Synechococcus*

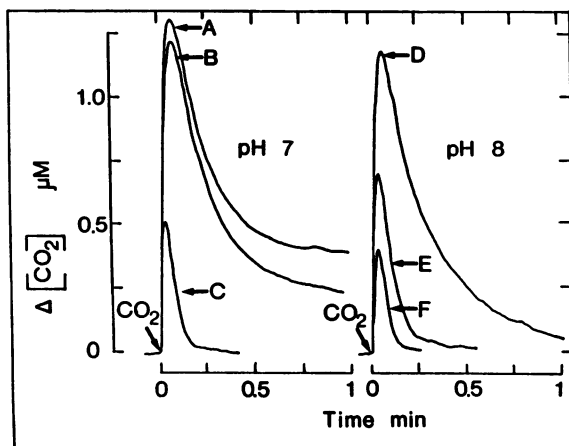


Figure 5. Effect of pH on the inhibition of active CO₂ transport by Na₂S. Cells (6.5–7.0 μg Chl · mL⁻¹) were incubated in 25 mM BTP/HCl buffer, containing 25 mM NaCl, at pH 7.03 (A–C) or pH 8.0 (D–F) for several minutes. The cells were subsequently pulsed with CO₂ in the dark (A, D) or light (C, F) and the changes in [CO₂] recorded. The difference between curve A and C (pH 7) or D and F (pH 8) was taken as the control level for CO₂ uptake in the absence of Na₂S. The effect of 30 μM Na₂S on CO₂ transport at pH 7.03 and 8.0 is shown by curve B and E respectively. The ratio of H₂S:HS⁻ at pH 7.03 and 8.0 was 0.76:1 and 0.081:1.

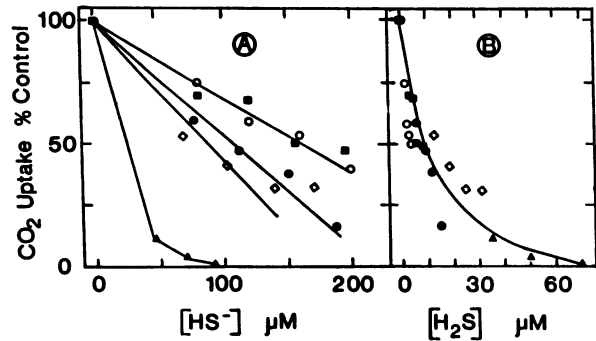


Figure 6. Effect of HS⁻ and H₂S concentration on active CO₂ transport by *Synechococcus*. Experiments similar to those shown in Figure 5 were conducted at pH 7.03 (▲), pH 7.65 (◇), pH 8.0 (●), pH 8.36 (■), and pH 8.70 (○) over a range of [Na₂S] from 0 to 200 μM. CO₂ transport ability was measured by the pulsing technique and CO₂ uptake was estimated in relationship to the control as described in the legend to Figure 3. The data were plotted either as a function of [HS⁻] (A) or [H₂S] (B). These concentrations were calculated using a pK_a for H₂S of 6.91 at 30°C. The [Chl] ranged from 7.0 to 8.3 μg · mL⁻¹.

leopoliensis UTEX 625 but does not appear to significantly affect the Na⁺-dependent HCO₃⁻ transport system (Fig. 1). The occurrence of HCO₃⁻ transport in the presence of H₂S was apparent from measurements of the yield of Chl *a* fluorescence (Fig. 1), which has been shown to be sensitive to variation in HCO₃⁻ transport (15, 17, 18), and from rates of photosynthesis that could not be sustained by CO₂ production from the dehydration of HCO₃⁻ (Fig. 1). In a recent study, we have confirmed that Chl *a* fluorescence quenching monitors inorganic carbon accumulation by direct measurements using the silicone fluid centrifugation technique (19). Independent evidence for the occurrence of HCO₃⁻ transport was provided by the observation that the [CO₂] in the medium rose to a level far in excess of its equilibrium at a time when photosynthesis was causing a net reduction in [DIC] in the medium (Figs. 1 and 2). Thus, HCO₃⁻ must serve both as the source of inorganic carbon for photosynthesis and for the newly arising CO₂ in the medium.

Photosynthetic carbon assimilation was not greatly changed by the [H₂S] used in our experiments as evidenced by the near normal rates of O₂ evolution (Fig. 1). Photosynthetic electron transport was also not greatly affected by these concentrations (Fig. 1). Higher [Na₂S] (300 μM), however, did cause significant reductions (30%) in the rate of O₂ evolution and Chl *a* fluorescence yield (not shown), in accord with the known inhibitory effect of H₂S (24).

Hydrogen sulfide is also known to inhibit CA from plant and animal sources (5, 12) and, while we cannot exclude this occurrence in our system, it is important to note that intracellular dehydration of HCO₃⁻ to CO₂ occurred at sufficient rate to sustain near normal rates of CO₂ fixation. In addition, the CO₂ which was observed to arise in the medium with H₂S poisoned cells (Figs. 1 and 2) depended upon intracellular dehydration of HCO₃⁻ since no catalyst of the reaction is present outside the cells (6). The collective data thus provide a strong case for the selective inhibition of CO₂ transport by H₂S without significant deleterious side effects to the photosynthetic apparatus, at least over the short term.

CO₂ Efflux

The rapid rise in [CO₂] above equilibrium caused by H₂S treatment required both millimolar levels of Na⁺ and energy input (Fig. 2). The requirement for Na⁺ reflects the Na⁺ requirement for active HCO₃⁻ transport (6, 8, 11, 13, 20). It appears, therefore, that active HCO₃⁻ transport into the cell followed by intracellular conversion to CO₂ and its leakage back into the medium along a concentration gradient is the mechanism responsible for the rise in extracellular [CO₂]. This view is supported by experiments with DI¹³C which showed that recently transported H¹³CO₃⁻ was the immediate source for ¹³CO₂ appearing in the medium. Consequently, a H₂S induced stimulation of dark respiration or release of a bound intracellular pool of DIC cannot account for the observed phenomenon.

In the absence of H₂S the CO₂ that leaks from the cell is transported efficiently back into the cell thereby keeping the steady state concentration near zero. Hydrogen sulfide, by blocking active CO₂ transport, simply reveals the ongoing leakage. It is possible that H₂S, rather than inhibiting CO₂ transport, brings about an increase solely in the leakage pathway for CO₂ with a concomitant change in the balance between transport and efflux. This possibility seems unlikely for several reasons. First, if this was the case, H₂S would not be expected to greatly reduce the initial rate of CO₂ uptake (Fig. 4B). Second, the effect of H₂S on the apparent uptake of CO₂ should be greatly reduced at low [Na⁺] since both the CO₂ gradient between the cells and the medium and the amount of effluxed CO₂ available for re-transport is significantly lower. Experiments show, however, that H₂S is a more potent inhibitor of CO₂ transport in the absence of Na⁺ and a large pool of intracellular DIC (Fig. 5, inset). Third, we have found that the transport of COS, a metabolized structural analog of CO₂, by the CO₂ transport system is inhibited by H₂S (19). Since no appreciable intracellular pool of COS is formed, and given that much of the COS within the cell is hydrolyzed, it would appear that the H₂S acts by directly preventing the uptake of COS (19). The effects of COS (19) and H₂S (Figs. 2–4) on CO₂ transport and efflux are remarkably similar and this strongly suggests that the site of action of H₂S is within the CO₂ transport system.

Lipid membranes are highly permeable to CO₂ and a considerable efflux of CO₂ from the cell would, in fact, be expected given the large Δ[CO₂] across the membrane (17). However, in a marine species of *Synechococcus*, membrane conductance to CO₂ was found to be quite low (10⁻⁵ cm · s⁻¹) compared to other biological membrane systems (3). In spite of this, efflux of CO₂ was readily observed to occur during HCO₃⁻ transport (2, 3). With *Synechococcus* UTEX 625, no observable CO₂ efflux occurred under normal conditions (Fig. 4C; 7, 17). This may be explained by the efficient transport of leaked CO₂ back into the cell in addition to a low membrane conductance to CO₂. A high affinity transport system for CO₂ (K_{1/2} [CO₂] = 0.2–0.4 μM) has been demonstrated in *Synechococcus* UTEX 625 (G Espie, A Miller, D Calvin, unpublished data). An obvious physiological role for the CO₂ transport system in photosynthesis, therefore, is to scavenge leaked CO₂. Since 'leaked' CO₂ arises primarily from HCO₃⁻

dehydration (with OH⁻ remaining in the cell), this leakage would cause a considerable burden on the mechanism for intracellular pH regulation without any attendant benefit to carbon metabolism. Return of the leaked CO₂ to the cell would at least benefit carbon metabolism, although at an additional cost to the energy budget of the cell. In addition, preventing the loss of recently transported DIC to the surroundings would enhance the competitive ability of these organisms when the extracellular [DIC] is low or limiting for growth. This is not to say that the only role of the CO₂ transport system is as a scavenger. It should be noted that the CO₂ transport system has sufficient capacity to support maximum rates of photosynthesis over a wide range of [DIC] when the supply of CO₂ is not limiting (8, 13) and thus is a major route for carbon entry into the cell at acidic pH. Furthermore, CO₂ transport appears to be the major means of carbon acquisition in high CO₂ grown cells of *Synechococcus* UTEX 625 (14) and PCC 6301 (4).

H₂S Inhibition and the Mechanism of CO₂ Uptake

Our analysis indicated that H₂S was the active species involved in inhibiting the CO₂ transport system. This was inferred from the observation that similar H₂S concentrations had an equivalent inhibitory effect over a range of extracellular pH values (Figs. 5 and 6). We assumed, however, that the dissociation of H₂S was the sole factor involved in the changing degree of inhibition of Na₂S (Figs. 5 and 6). If, in addition, an activity-linked titratable group existed at the site of inhibition, this would provide an additional level of complexity to the analysis. Our data, therefore, cannot exclude some involvement of the HS⁻ ion, either directly or indirectly in the inhibition of CO₂ transport.

Hydrogen sulfide and COS (19) inhibited CO₂ transport much more effectively than HCO₃⁻ transport in *Synechococcus* UTEX 625. Considerable care, however, must be taken when using COS since intact cells, added CA and/or alkaline pH cause the hydrolysis of COS to H₂S and CO₂ (19). The effects of H₂S and COS on CO₂ uptake and the induction of CO₂ efflux are remarkably similar and in both cases inhibition of CO₂ transport is independent of the occurrence of HCO₃⁻ transport or the presence of millimolar concentrations of Na⁺. In addition, H₂S and COS both act rapidly (within 15 s) and the effects are reversible, at least over exposure times up to 5 min. Concentrations of COS as low as 3 μM inhibit CO₂ transport with maximal effects occurring at 30 to 40 μM at pH 8 (19). This level of H₂S, however, only brings about partial inhibition at pH 8. Presently, this difference in concentration requirement is the only means to distinguish between H₂S and COS inhibition.

Inhibition of CO₂ transport by COS in *Synechococcus* PCC 7942 has also been reported by Ogawa and Togasaki (23). In most experiments cells were incubated for at least 10 min with COS in the light prior to experimentation. If this organism hydrolyzes COS as does *Synechococcus* UTEX 625, then a large part of the observed inhibition of CO₂ transport may be due to H₂S rather than COS. To minimize such complications, it is essential to use low concentration of COS, short incubation and assay times, and to avoid the use of conditions which accelerate COS hydrolysis.

The means by which H₂S inhibits CO₂ transport is unclear. Like CO₂ and COS, H₂S is a small planar molecule, but its electronic structure, bond angles, and chemical properties are distinctly different. For these reasons it seems unlikely that H₂S functions as an analog inhibitor or as an alternate substrate for the CO₂ transport system. Indeed, within the mass spectrometer detection limits we have not observed carrier-mediated uptake of H₂S.

Also, hydrogen sulfide is a well known metal complexing agent and it is this property which accounts for its efficient inhibition of the Zn containing enzyme CA (5, 12). Both H₂S and HS⁻ inhibit CA although through somewhat different reaction sequences (5). In either case the final form of the enzyme is one in which the bisulfide ion is bound to the catalytically essential Zn atom (5). By analogy to the effect of H₂S on CA, it is tempting to ascribe a role for a divalent metal ion in the transport of CO₂. Two likely candidates are Zn and Co, both of which endow the CA apoenzyme with catalytic activity (5). The rapid restoration of transport activity upon the removal of H₂S suggests a weak interaction between H₂S and the site of inhibition. Additional investigations using specific metal complexing agents, however, will be necessary to provide further insight into the possible role of a divalent metal in the active transport of CO₂.

Previous studies have suggested the participation of a membrane-bound CA-like moiety in the transport of CO₂ by *Anabaena variabilis*, *Anacystis nidulans* R2, and *Synechococcus* PCC 7942 (1, 22, 25, 28). This conclusion was largely based on the observation that EZ inhibited CO₂ transport (1, 22, 25, 28) without apparent inhibition of intracellular CA (25). Inhibition of CO₂ transport by H₂S in *Synechococcus* UTEX 625 further strengthens the view that CA and the CO₂ transport system have properties in common. Furthermore, like H₂S, EZ inhibits CA by binding to the catalytically essential Zn and this is its only known means of inhibition (5). Unlike H₂S, however, EZ is an intrinsically poor metal complexing agent (5). Rather, the high affinity binding of EZ to CA depends both upon the presence of the correct metal at the active site and the binding of the side chain to the enzyme which brings the sulfonamide group close to the Zn (5). Consequently, a common mechanism may exist for the inhibition of CO₂ transport by H₂S and EZ.

In *Anabaena*, the suggested role of the CA-like moiety is to convert CO₂ to HCO₃⁻ within the membrane for subsequent transport into the cell by the HCO₃⁻ transport system (1, 22, 28). In *Synechococcus* PCC 7942, however, it has been proposed that HCO₃⁻ from the medium is converted to CO₂ within the membrane by a 'front end mechanism' and that this CO₂ is then used as a substrate for the CO₂ transport system (4, 25). Both the CO₂ delivered by the front end mechanism and CO₂ taken up directly from the medium are converted to HCO₃⁻ by a CA-like function of the CO₂ transport system during passage across the membrane (25). Thus, in the former case CO₂ uptake is obligately dependent upon a HCO₃⁻ transport system while, in the latter case, HCO₃⁻ uptake is obligately dependent upon a CO₂ transport system. Neither of these arrangements adequately describes the relationship between CO₂ and HCO₃⁻ transport in *Synechococcus* UTEX 625, however. In previous studies we have shown that

CO₂ transport occurred in the absence of HCO₃⁻ uptake (7, 8, 13, 15) while this and a companion study (19) demonstrated that HCO₃⁻ transport occurred normally under conditions where CO₂ transport was greatly impaired. The physiological separation of these transport activities into discrete events indicates that CO₂ and HCO₃⁻ are transported into the cell by separate, independent systems (Fig. 7). Whether the CO₂ or HCO₃⁻ transport systems of *Synechococcus* UTEX 625 actually catalyze a CA-like hydration/dehydration reaction in addition to or as part of their transport function remains an open question.

A Model for DIC Transport

A schematic diagram depicting the relationship between the CO₂ and HCO₃⁻ transport systems of *Synechococcus* UTEX 625 is shown in Figure 7. This model differs from previous models (1, 22, 25, 28) in that the CO₂ and HCO₃⁻ transport systems are considered to be separate, specific, and independent. As discussed here and elsewhere (7, 8, 13, 19) evidence for this arrangement is provided primarily from studies with selective inhibitors. For example, transport of HCO₃⁻ by *Synechococcus* was completely inhibited by depriving the cells of millimolar concentrations of Na⁺ (6, 7, 8, 13) and by Li⁺ (8, 13) or monensin (18) in the presence of Na⁺. None of these treatments caused a significant reduction in CO₂ transport. Furthermore, the initiation of HCO₃⁻ transport by Na⁺ addition in inhibited cells also had no apparent effect on CO₂ transport (7). Similarly, when CO₂ transport was inhibited by H₂S (Fig. 1) or COS (19) sufficient Na⁺-dependent HCO₃⁻ transport activity remained to support almost normal rates of photosynthesis. The concept of two distinct transport systems is further supported by the following observations. First, carbonic anhydrase stimulated intracellular DIC accumulation and photosynthesis in cells in which the Na⁺-dependent HCO₃⁻ transport system was inhibited by Li⁺ or by lack of Na⁺ (8, 13), thus demonstrating the existence

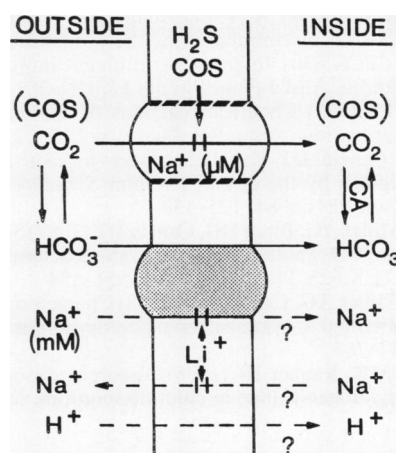


Figure 7. A schematic model for CO₂ and HCO₃⁻ transport in *Synechococcus* UTEX 625. Transport of CO₂ is inhibited by H₂S and COS. Transport of HCO₃⁻ is inhibited by Li⁺ and monensin. Monensin collapses the Na⁺ gradient through an electroneutral exchange with H⁺ and is therefore unlikely to act directly on the HCO₃⁻ transport system. Both CO₂ and HCO₃⁻ transport are stimulated by Na⁺.

of an alternate pathway for DIC acquisition. Second, cells grown on high CO₂ or DIC retained their ability to actively transport CO₂ but their capacity for HCO₃⁻ transport was greatly reduced or absent (4, 14). Finally, the optimum Na⁺ concentration for CO₂ and HCO₃⁻ transport differ by more than two orders of magnitude (8, 17).

The model shows both CO₂ and HCO₃⁻ arriving on the inner side of the membrane. It must be emphasized that this is speculative since no experimental data is available on the nature of the products of the transport processes for *Synechococcus* UTEX 625. Regardless of the species that arrives inside the cell, HCO₃⁻ and CO₂ are rapidly interconverted within the cell (3, 27; our unpublished observations) so that the form of the product would not be important to subsequent photosynthesis. HCO₃⁻ transport and utilization would, of course, require either OH⁻ exit or H⁺ uptake to maintain electrical balance and intracellular pH but the mechanism of this is not known.

Both H₂S and COS (19) appear to act directly on the CO₂ transport system but the site of action of Na⁺ and Li⁺ is not known. For convenience alone they are shown to act directly on HCO₃⁻ transport but this is subject to later modification.

ACKNOWLEDGMENT

We thank Mr. Douglas G. Birch for expert assistance in the operation of the mass spectrometer.

LITERATURE CITED

- Abe T, Tsuzuki M, Miyachi S (1987) Transport and fixation of inorganic carbon during photosynthesis in cells of *Anabaena* grown under ordinary air. III. Some characteristics of the HCO₃⁻ transport system in cells grown under ordinary air. *Plant Cell Physiol* **28**: 867-874
- Badger MR, Andrews TJ (1982) Photosynthesis and inorganic carbon usage by the marine cyanobacterium *Synechococcus* sp. *Plant Physiol* **70**: 517-523
- Badger MR, Bassett M, Comins HN (1985) A model for HCO₃⁻ accumulation and photosynthesis in the cyanobacterium *Synechococcus* sp. Theoretical predictions and experimental observations. *Plant Physiol* **77**: 465-471
- Badger MR, Gallagher A (1987) Adaptation of photosynthetic CO₂ and HCO₃⁻ accumulation by the cyanobacterium *Synechococcus* PCC 6301 to growth at different inorganic carbon concentrations. *Aust J Plant Physiol* **14**: 189-201
- Coleman JE (1975) Chemical reactions of sulfonamides with carbonic anhydrase. *Annu Rev Pharmacol* **15**: 221-242
- Espie GS, Canvin DT (1987) Evidence for Na⁺-independent HCO₃⁻ uptake by the cyanobacterium *Synechococcus leopoliensis*. *Plant Physiol* **84**: 125-130
- Espie GS, Miller AG, Birch DG, Canvin DT (1988) Simultaneous transport of CO₂ and HCO₃⁻ by the cyanobacterium *Synechococcus* UTEX 625. *Plant Physiol* **87**: 551-554
- Espie GS, Miller AG, Canvin DT (1988) Characterization of the Na⁺ requirement in cyanobacterial photosynthesis. *Plant Physiol* **88**: 757-763
- Goldhaber MB, Kaplan IR (1975) Apparent dissociation constants of hydrogen sulfide in chloride solutions. *Mar Chem* **3**: 104
- Kaplan A, Badger MR, Berry JA (1980) Photosynthesis and intracellular inorganic carbon pool in the blue-green alga *Anabaena variabilis*: Response to external CO₂ concentration. *Planta* **149**: 219-226
- Kaplan A, Volokita M, Zenvirth D, Reinhold L (1984) An essential role for sodium in the bicarbonate transporting system of the cyanobacterium *Anabaena variabilis*. *FEBS Lett* **176**: 166-168
- Maren TH, Sanyal G (1983) The activity of sulfonamides and anions against the carbonic anhydrases of animals, plants and bacteria. *Annu Rev Pharmacol Toxicol* **23**: 439-459
- Miller AG, Canvin DT (1985) Distinction between HCO₃⁻ and CO₂-dependent photosynthesis in the cyanobacterium *Synechococcus leopoliensis* based on the selective response of HCO₃⁻ transport to Na⁺. *FEBS Lett* **187**: 29-32
- Miller AG, Canvin DT (1987) Na⁺-stimulation of photosynthesis in the cyanobacterium *Synechococcus* UTEX 625 grown on high levels of inorganic carbon. *Plant Physiol* **84**: 118-124
- Miller AG, Canvin DT (1987) The quenching of chlorophyll *a* fluorescence as a consequence of the transport of inorganic carbon by the cyanobacterium *Synechococcus* UTEX 625. *Biochim Biophys Acta* **894**: 407-413
- Miller AG, Colman B (1980) Active transport and accumulation of bicarbonate by a unicellular cyanobacterium. *J Bacteriol* **143**: 1253-1259
- Miller AG, Espie GS, Canvin DT (1988) Active transport of CO₂ by the cyanobacterium *Synechococcus* UTEX 625. Measurement by mass spectrometry. *Plant Physiol* **86**: 677-683
- Miller AG, Espie GS, Canvin DT (1988) Chlorophyll *a* fluorescence yield as a monitor of both active CO₂ and HCO₃⁻ transport by the cyanobacterium *Synechococcus* UTEX 625. *Plant Physiol* **86**: 655-658
- Miller AG, Espie GS, Canvin DT (1989) Use of carbon oxysulfide, a structural analog of CO₂, to study active CO₂ transport in the cyanobacterium *Synechococcus* UTEX 625. *Plant Physiol* **90**: 1221-1231
- Miller AG, Turpin DH, Canvin DT (1984) Na⁺ requirement for growth, photosynthesis and pH regulation in the alkalotolerant cyanobacterium *Synechococcus leopoliensis*. *J Bacteriol* **159**: 100-106
- Millero FJ, Plese T, Fernandez M (1988) The dissociation of hydrogen sulfide in seawater. *Limnol Oceanogr* **33**: 269-274
- Ogawa T, Kaplan A (1987) The stoichiometry between CO₂ and H⁺ fluxes involved in the transport of inorganic carbon in cyanobacteria. *Plant Physiol* **83**: 888-891
- Ogawa T, Togasaki RK (1988) Carbonyl sulfide: An inhibitor of inorganic carbon transport in cyanobacteria. *Plant Physiol* **88**: 800-804
- Padan E (1979) Facultative anoxygenic photosynthesis in cyanobacteria. *Annu Rev Plant Physiol* **30**: 27-40
- Price GD, Badger MR (1989) Ethoxycarbonyl inhibition of CO₂ uptake in the cyanobacterium *Synechococcus* PCC 7942 without apparent inhibition of internal carbonic anhydrase activity. *Plant Physiol* **89**: 37-43
- Schreiber U, Schliwa U, Bilger W (1986) Continuous recording of photochemical and non-photochemical fluorescence quenching with a new type of modulation fluorometer. *Photosynth Res* **10**: 51-62
- Tu CK, Spiller H, Wynns GC, Silverman DN (1987) Carbonic anhydrase and the uptake of inorganic carbon by *Synechococcus* (UTEX 2380). *Plant Physiol* **85**: 72-77
- Volokita M, Zenvirth D, Kaplan A, Reinhold L (1984) Nature of the inorganic carbon species actively taken up by the cyanobacterium *Anabaena variabilis*. *Plant Physiol* **76**: 599-602